



HAL
open science

Lean regional muscle volume estimates using explanatory bioelectrical models in healthy subjects and patients with muscle wasting

Damien Bachasson, Alper Carras Ayaz, Jessie Mosso, Aurélie Canal, Jean-Marc Boisserie, Ericky C A Araujo, Olivier Benveniste, Harmen Reyngoudt, Benjamin Marty, Pierre G Carlier, et al.

► To cite this version:

Damien Bachasson, Alper Carras Ayaz, Jessie Mosso, Aurélie Canal, Jean-Marc Boisserie, et al.. Lean regional muscle volume estimates using explanatory bioelectrical models in healthy subjects and patients with muscle wasting. *Journal of Cachexia, Sarcopenia and Muscle*, 2020, 12 (1), pp.39-51. 10.1002/jcsm.12656 . hal-03146449

HAL Id: hal-03146449

<https://hal.sorbonne-universite.fr/hal-03146449>

Submitted on 19 Feb 2021

HAL is a multi-disciplinary open access archive for the deposit and dissemination of scientific research documents, whether they are published or not. The documents may come from teaching and research institutions in France or abroad, or from public or private research centers.

L'archive ouverte pluridisciplinaire **HAL**, est destinée au dépôt et à la diffusion de documents scientifiques de niveau recherche, publiés ou non, émanant des établissements d'enseignement et de recherche français ou étrangers, des laboratoires publics ou privés.

Lean regional muscle volume estimates using explanatory bioelectrical models in healthy subjects and patients with muscle wasting

Damien Bachasson^{1*} , Alper Carras Ayaz¹, Jessie Mosso¹, Aurélie Canal¹, Jean-Marc Boisserie^{2,4}, Ericky C.A. Araujo^{2,4} , Olivier Benveniste³ , Harmen Reingoudt^{2,4} , Benjamin Marty^{2,4} , Pierre G. Carlier^{2,4}  & Jean-Yves Hogrel¹ 

¹Institute of Myology, Neuromuscular Investigation Center, Neuromuscular Physiology and Evaluation Laboratory, Paris, France, ²Institute of Myology, Neuromuscular Investigation Center, NMR Laboratory, Paris, France, ³Department of Internal Medicine and Clinical Immunology and Inflammation-Immunopathology-Biotherapy Department (I2B), Pitié-Salpêtrière University Hospital, Assistance Publique-Hôpitaux de Paris, East Paris Neuromuscular Diseases Reference Center, Inserm U974, Sorbonne Université, Paris, France, ⁴CEA, DRF, IBFJ, MIRcen, NMR Laboratory, Paris, France

Abstract

Background The availability of non-invasive, accessible, and reliable methods for estimating regional skeletal muscle volume is paramount in conditions involving primary and/or secondary muscle wasting. This work aimed at (i) optimizing serial bioelectrical impedance analysis (S_{BIA}) by computing a conductivity constant based on quantitative magnetic resonance imaging (MRI) data and (ii) investigating the potential of S_{BIA} for estimating lean regional thigh muscle volume in patients with severe muscle disorders.

Methods Twenty healthy participants with variable body mass index and 20 patients with idiopathic inflammatory myopathies underwent quantitative MRI. Anatomical images and fat fraction maps were acquired in thighs. After manual muscle segmentation, lean thigh muscle volume (IV_{MRI}) was computed. Subsequently, multifrequency (50 to 350 kHz) serial resistance profiles were acquired between current skin electrodes (i.e. ankle and hand) and voltage electrodes placed on the anterior thigh. *In vivo* values of the muscle electrical conductivity constant were computed using data from S_{BIA} and MRI gathered in the right thigh of 10 healthy participants. Lean muscle volume (IV_{BIA}) was derived from S_{BIA} measurements using this newly computed constant. Between-day reproducibility of IV_{BIA} was studied in six healthy participants.

Results Electrical conductivity constant values ranged from 0.82 S/m at 50 kHz to 1.16 S/m at 350 kHz. The absolute percentage difference between IV_{BIA} and IV_{MRI} was greater at frequencies >270 kHz ($P < 0.0001$). The standard error of measurement and the intra-class correlation coefficient for IV_{BIA} computed from measurements performed at 155 kHz (i.e. frequency with minimal difference) against IV_{MRI} were 6.1% and 0.95 in healthy participants and 9.4% and 0.93 in patients, respectively. Between-day reproducibility of IV_{BIA} was as follows: standard error of measurement = 4.6% (95% confidence interval [3.2, 7.8] %), intra-class correlation coefficient = 0.98 (95% confidence interval [0.95, 0.99]).

Conclusions These findings demonstrate a strong agreement of lean muscle volume estimated using S_{BIA} against quantitative MRI in humans, including in patients with severe muscle wasting and fatty degeneration. S_{BIA} shows promises for non-invasive, fast, and accessible estimation and follow-up of lean regional skeletal muscle volume for transversal and longitudinal studies.

Keywords Skeletal muscle; Bioelectrical impedance analysis; Myopathies; Muscle mass; Muscle volume; Muscle atrophy; Muscle fatty infiltration

Received: 22 May 2020; Revised: 22 September 2020; Accepted: 5 November 2020

*Correspondence to: Damien Bachasson, PT, PhD, Institute of Myology, Neuromuscular Investigation Center, Neuromuscular Physiology and Evaluation Laboratory, Hôpital Universitaire Pitié Salpêtrière, Paris 75651 cedex 13, France. Tel: +33 1 42 16 66 41, Fax: +33 1 42 16 58 81, Email: d.bachasson@institut-myologie.org

Introduction

The availability of accessible, non-invasive, and robust methods for estimating skeletal muscle volume (SMV) is paramount for clinicians and scientists within various physiological and pathophysiological contexts involving muscle remodelling. Regional SMV, and more specifically thigh SMV, has emerged as an important hallmark across the health care continuum.^{1–3}

Methods for estimating regional SMV in humans are numerous and rely on a wide range of physical principles, models, and assumptions.^{4,5} Dual-energy X-ray absorptiometry (DXA) is the most widespread technique for assessing lean regional SMV. DXA has many strengths (e.g. small radiation dose and cheaper than other imaging techniques), but as a two-dimensional imaging technique, regional SMV estimates are obtained indirectly using anatomical models.^{4,5} Computerized tomography (CT) and magnetic resonance imaging (MRI) are recognized as the gold standards for regional body composition analysis.^{4,6} As three-dimensional imaging techniques, CT and MRI can be used to obtain precise estimates of regional SMV. As opposed to CT, MRI is non-ionizing, rendering it the safe alternative for three-dimensional volumetric acquisitions. Importantly, CT and MRI can also determine intramuscular fat content, which is a critical information in conditions such as myopathies and sarcopenia. However, both CT and MRI require the segmentation of different tissue compartments within images that is known to be a very labour-intensive task. Automated or semi-automated approaches have been proposed, but they remain difficult to apply when severe degenerative muscle changes take place.^{4,7} Consequently, when a simple estimate of lean regional SMV is being sought, limitations in the use of CT and MRI are largely related to their high costs and the technical expertise required to acquire and process images.

Bioimpedance measurements refer to all methods based on the characterization of the passive electrical properties of biological tissues in response to the injection of an external current.⁸ Methods referred to as bioelectrical impedance analysis (BIA) have been identified as non-invasive, non-irradiant, cost-effective, and portable for the assessment of appendicular SMV.^{8–10} However, BIA has been mostly performed using descriptive models that rely on poorly generalizable sample-specific regression equations.^{8,9} Although these models may be sufficient in epidemiological studies, the current consensus stresses that these approaches may be used with caution when precise individual measurements of body composition are pursued.⁴ Other local approaches referred to as electrical impedance myography may allow to discriminate pathological muscle status and change over time using a set of non-specific parameters but do not provide estimates of regional SMV.^{11,12}

A considerably smaller amount of studies has proposed explanatory BIA models for the estimation of regional

SMV.^{13–16} Brown *et al.* first introduced a method solely based on measured impedance and anthropometric measurements.¹³ Subsequently, Salinari *et al.* proposed an elegant approach for estimating whole-limb SMV based on the resistance profile of the whole limb.^{15,16} For clarity, this approach is referred to as serial bioelectrical impedance analysis (S_{BIA}) in this work. Excellent consistency between S_{BIA} and DXA in the lower limb of normal-weight and overweight healthy subjects has been reported (i.e. relative error was $<7 \pm 3\%$).¹⁶ Salinari *et al.* also reported good consistency between S_{BIA} and MRI (with no assessment of intramuscular fat) in the lower limb in a small group of male healthy subjects ($n = 6$; i.e. relative error was $<6 \pm 4\%$),¹⁵ and these findings were confirmed in 15 healthy men in a study conducted by Stahn *et al.*¹⁷ To the best of our knowledge, there are no S_{BIA} data available in women. Stahn *et al.*¹⁷ reported higher accuracy of estimates of lower limb SMV when using higher frequencies (i.e. 500 kHz). However, the potential advantage of multifrequency acquisitions within such models remains to be scrutinized. The value of the muscle conductivity constant is the most critical aspect of these models. In previous works,^{15–17} the authors used published muscle conductivity constants^{18–21} so that uncertainties regarding true *in vivo* values of skeletal muscle conductivity remain. Whether these models may be applicable in patients with severe muscle wasting associated with degenerative changes, in particular, intramuscular fat infiltration, has never been investigated. Although using a relatively small number of measurements over the whole lower limb has been reported to provide reasonable estimates,¹⁶ it remains unclear whether these models could be applied within shorter segments such as the thigh in both healthy subjects and patients with muscle impairments. Another aspect that has never been investigated is the between-day reproducibility of S_{BIA} measurements.

Therefore, the aims of the present study were (i) to optimize S_{BIA} numerical models by computing a conductivity constant based on actual thigh structure as assessed using state-of-the-art quantitative MRI, (ii) to investigate its ability to estimate lean thigh muscle volume in healthy participants, and patients (men and women) with muscle wasting and degenerative changes such as intramuscular fatty infiltration, (iii) to investigate the potential advantage of multifrequency S_{BIA} acquisitions, and (iv) to assess the between-day reproducibility of S_{BIA} .

Methods

Participants and study design

Patients with a confirmed diagnosis of inclusion body myositis and unmatched healthy participants with variable body mass

index (BMI) and physical fitness level were proposed to participate in this study. All participants gave written informed consent. This study conformed to the Declaration of Helsinki and was approved by the local ethics committee. Participants were advised to refrain from alcohol and exercise for 48 h before measurements and to refrain from smoking and the consumption of caffeinated beverages on the day of measurement. No specific instructions regarding hydration prior measurements were given to participants. Participants underwent MRI followed by S_{BIA} measurements within a single visit. A subsample of six healthy participants was studied for between-day reproducibility of S_{BIA} measurements within a second visit 24 to 72 h apart.

Magnetic resonance imaging acquisitions and processing

Participants underwent an MRI scan of the thighs using a 3 T scanner (Prisma^{Fit}, Siemens, Healthineers, Erlangen, Germany). Scans were performed with subjects lying feet-first in the supine position. The body coil was used for RF transmission, and a body matrix coil positioned on the thighs was operated in conjunction with a spine matrix integrated into the patient table for signal reception. Axial images were acquired using a 3D gradient echo sequence with the following parameters: echo times = 2.75, 3.95, and 5.15 ms; repetition time = 10 ms; flip angle = 3°; field of view = 224 × 448 × 320 mm³; spatial resolution = 1 × 1 × 5 mm³; and acquisition time = 5 min 38 s. The centre slice was positioned at one-third of the distance between the upper edge of the patella and the anterior–superior iliac spine (ASIS). The centre of the central slice was carefully skin marked. Water and fat maps were obtained using a standard three-point Dixon reconstruction, and fat fraction (FF) maps were computed as the ratio between the fat signal and the sum of the water and fat signals.²²

Magnetic resonance imaging analysis

Out-of-phase Dixon images were manually segmented using the ITK-Snap software according to four distinct areas labelled as follows: anterior muscle compartment (i.e. quadriceps), posterior muscle compartment (i.e. hamstrings and adductors), bone, and subcutaneous tissue associated with neurovascular bundles and intermuscular tissues. Segmentation was performed every 4 cm (i.e. every eight slices) as previously reported to yield accurate estimates of muscle volume.²³ For each slice, the whole muscle cross-sectional area (CSA_{MRI}) was computed and the lean muscle cross-sectional area ($ICSA_{MRI}$) was obtained by removing the contribution of adipose tissue using FF maps.²⁴ Subsequently, values for CSA_{MRI} and $ICSA_{MRI}$ were fitted using cubic spline

interpolation for computing volumes. Finally, overall values for muscle volume (V_{MRI}) and lean muscle volume (IV_{MRI}) were computed over a length corresponding to 40% of the distance between the patella–ASIS, centred on the central slice, and retrieved using standard trapezoidal integration. Therefore, the studied anatomical region was similar in every individual subject. An overview of image segmentation is displayed in *Figure 1*.

Serial bioelectrical impedance measurements

Measurements were performed using a commercialized multifrequency bioimpedance device (Z-Scan, Bioparhom, France) allowing raw impedance data acquisition. The participants were lying supine for 10 min before measurements to allow fluids to equilibrate. To avoid any short circuits, participants were asked to keep their arms alongside their body, a few centimetres away from it, and to slightly spread their legs to avoid any contact between them. Before applying the electrodes, the skin was shaved and rubbed with 70% ethanol. Conventional AgCl/Ag electrodes (Meditrace 100; Kendall, Mansfield, MA) were used for both current injection and measurement. Low-intensity (70 µA) alternative current was sent through injection electrodes positioned in the centre of the third metacarpal of the hand and slightly above the lateral malleolus. A reference voltage electrode was positioned on the forearm, 15 cm away from the wrist injection electrode. The first voltage electrode was positioned on the anterior part of the thigh at the level of the skin mark corresponding to the central MRI slice (see above). Other voltage electrodes were positioned proximally and distally from the central mark with 4 cm intervals. All thigh voltage electrodes were connected to an electronic multiplexer (MAX306CPI+, Maxim Integrated, San Jose, CA 95134, USA) driven by a microcontroller (Arduino Uno) allowing the automatic switch of the voltage electrode along the thigh. Multifrequency measurements were performed from 50 to 350 kHz, with a 5 kHz step. An overview of the experimental set-up is displayed in *Figure 2*. The duration of the acquisition was 30 s per voltage electrode measurement and less than 5 min per side when considering all measurements.

Serial bioelectrical impedance analysis

Computation of muscle cross-sectional area and volume

As the longitudinal conductivity of the muscle is much higher than other tissues and because the contribution of reactance is anticipated to be negligible within the range of tested frequencies, the injected current flow in the longitudinal direction through the thigh was assumed to be mostly carried by the resistive component of muscle tissue.¹⁷ Therefore, only the real part of the impedance (reflecting the resistance)

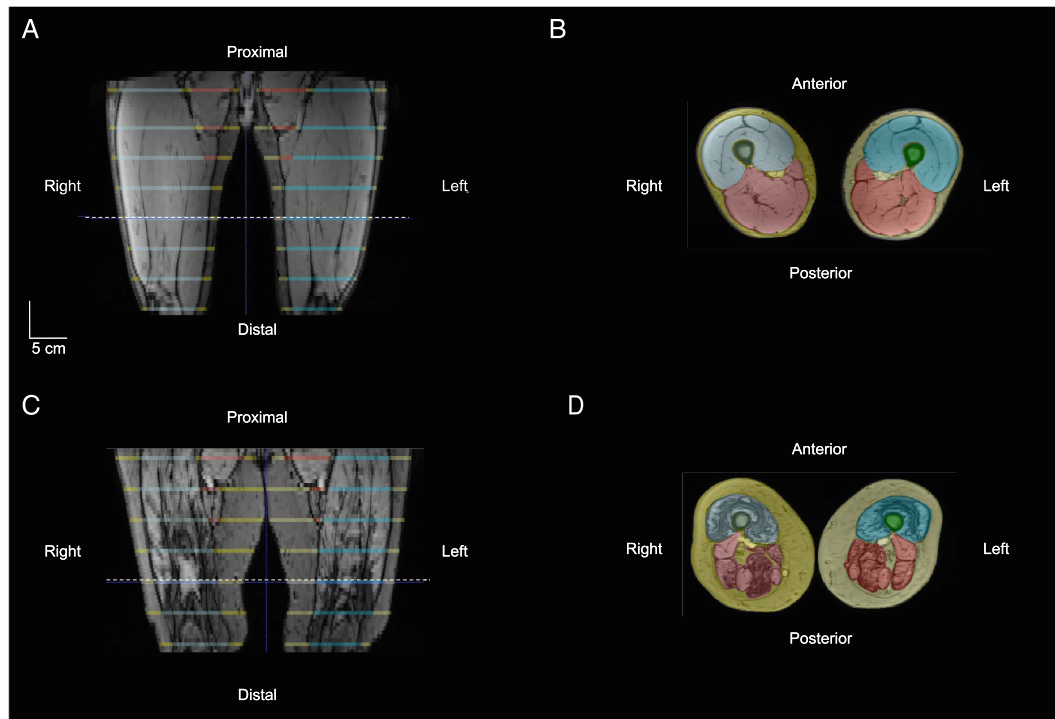


Figure 1 Typical quantitative magnetic resonance imaging acquisitions and processing. Illustration of the positioning of segmented slices in thighs in the coronal plane in one healthy participant (Panel A) and one patient (Panel C). Example how the regions of interest were drawn in the transverse plane the out-of-phase Dixon images depicted by the white dotted line in Panels (A)–(C) (Panel B for the healthy participant and Panel D for the patient): subcutaneous fat tissue–neurovascular bundles–intermuscular tissue (yellow), anterior muscle compartment (red), posterior muscle compartment (i.e. hamstrings and adductors, blue), and bone (green).

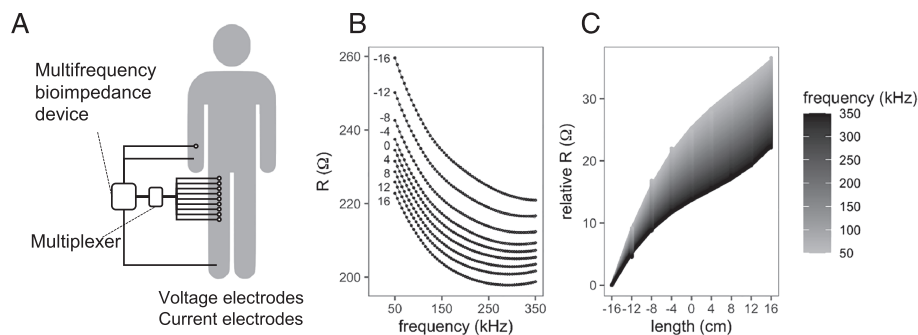


Figure 2 Experimental set-up for serial bioelectrical impedance measurements and typical measurements. Schematic of the experimental set-up (Panel A). Panel (B) shows resistance acquired at different frequencies between the hand voltage electrode and all voltage electrodes along the thigh (numbers represent the distance from the electrode corresponding to the central magnetic resonance imaging slice). Panel (C) shows the relative resistance profile along the thigh. The numbers on the left side of the curves indicate the distance from the first distal electrode above the patella. Lines represent resistance–frequency profiles fitted using a double exponential function with the Levenberg–Marquardt algorithm (Panel B) and relative resistance–length profile fitted using third-order polynomial function (Panel C; see text for more details).

was used in the analysis. To reduce potential artefacts in resistance measurements (e.g. caused by insufficient skin preparation, cable movement, patient movement, and imperfect skin–electrode contact), each resistance profile according to frequency was fitted using a double exponential function using the Levenberg–Marquardt algorithm (Figure 2B). The

number of thigh voltage electrodes used for S_{BIA} was adjusted depending on individual patella–ASIS distance. Relative resistance values were fitted using a constrained third-order polynomial function. The derivative of the relative resistance was computed. The lean cross-sectional area ($ICSA_{BIA}$) was computed as follows:

$$ICSA_{BIA} = \frac{1}{\left(\frac{\partial R}{\partial z}\right) \cdot \sigma}, \quad (1)$$

where $\frac{\partial R}{\partial z}$ is the electrical resistance gradient in Ω/m between two locations of the body part separated from a distance z (m) and σ the conductivity constant (S/m). As performed in MRI, lean thigh muscle volume (IV_{BIA}) was computed over a length corresponding to 40% of the distance between the patella–ASIS, centred on the electrode corresponding to the MRI central slice, and extracted using standard trapezoidal integration.

To investigate whether muscle volume can be estimated on shorter length using a reduced number of voltage electrodes, IV_{BIA} and corresponding IV_{MRI} values were also computed using five or three electrodes around the central slice corresponding to 30% and 14% of the patella–ASIS distance, respectively.

Computation of the muscle electrical conductivity constant

In vivo values of the muscle electrical conductivity constant were computed at all tested frequencies according to Equation 2 by using data from S_{BIA} and MRI gathered in the right thigh of randomly chosen healthy participants ($n = 10$, 5 men and 5 women).

$$\sigma = \frac{1}{\left(\frac{\partial R}{\partial z}\right) \cdot ICSA_{MRI}}. \quad (2)$$

This newly computed muscle conductivity constant was then used in both thighs for the analysis of S_{BIA} data of all healthy participants and patients studied.

Statistics

Data are shown as mean \pm standard deviation within text and figures. The assumptions of normality and sphericity were confirmed using the D'Agostino K -squared and Mauchly tests, respectively. For cross-validation of S_{BIA} measurements against MRI and between-day reproducibility of S_{BIA} measurements, regression analysis and Bland–Altman plots were performed. Difference in means and paired t -tests were used for the detection of systematic bias. The standard error of measurement (SEM) was used to study absolute reliability. Relative reliability was assessed using intra-class correlation coefficients ($ICC_{2,1}$). Linear mixed models were used to investigate the main effect and interaction of frequency and location of measurements along the thigh on absolute MRI– S_{BIA} differences for both areas and volumes. Tukey's post hoc tests were conducted when a significant main or interaction was found. Pearson's or Spearman's rank correlation coefficient was used for studying potential relationships between

normally or non-normal distributed variables, respectively. All analyses were performed in the computing environment R Version 3.2.3.²⁵ Statistical significance was set at $P < 0.05$ for all tests.

Results

Twenty healthy participants [8 women, age = 37 ± 9 years, BMI ranging from 16.8 to 31.3 kg/m²; 12 men, age 35 ± 10 years, BMI ranging from 19.8 to 26.2 kg/m²; with no significant age difference ($P = 0.65$)] and 20 patients diagnosed with inclusion body myositis [10 men, age = 63 ± 7 years, BMI = 26.7 ± 3.7 kg/m²; 10 women, age = 68 ± 10 years, BMI = 24.6 ± 9.4 kg/m²; with no significant age difference ($P = 0.96$)] were studied. Data from two patients were excluded from analysis because of aberrant S_{BIA} measurements caused by contact between legs and/or movements during acquisitions.

Quantitative magnetic resonance imaging

Areas of whole muscle, lean muscle, bone, and subcutaneous tissue associated with neurovascular bundles along the thigh extracted from MRI are displayed in *Figure 3*. Patients with neuromuscular disorders had lower overall and lean muscle volume than healthy participants (i.e. V_{MRI} was 1688 ± 491 vs. 2214 ± 698 cm³; $P < 0.001$). Within healthy participants, women had lower overall muscle volume (V_{MRI} was 1498 ± 202 vs. 2691 ± 43 cm³ in women and men, respectively; $P < 0.001$) and higher FF ($7.5 \pm 1.4\%$ vs. $4.9 \pm 1.0\%$ in women and men, respectively; $P < 0.001$). Patients exhibited various levels of muscle FF ($26.5 \pm 14.5\%$, range = 7.4–59.5%), and healthy participants exhibited low muscle FF ($5.9 \pm 1.8\%$, range = 3.2–10.9%). There was no difference in muscle volume or FF between men and women in the patient group (both $P > 0.29$).

Muscle conductivity constant and agreement between estimates obtained using serial bioelectrical impedance analysis and quantitative magnetic resonance imaging

Depending on individual thigh length, nine ($n = 20$), eight ($n = 17$), or seven ($n = 1$) thigh voltage electrodes were used for S_{BIA} measurements. The muscle conductivity constant as a function of frequency is displayed in *Figure 4*. It ranged from 0.82 S/m at 50 kHz to 1.16 S/m at 350 kHz. Absolute percentage differences between $ICSA_{BIA}$ and $ICSA_{MRI}$ ($\Delta ICSA$) according to measurement location along the thigh are displayed in *Figure 5A*. A significant main effect of measurement location

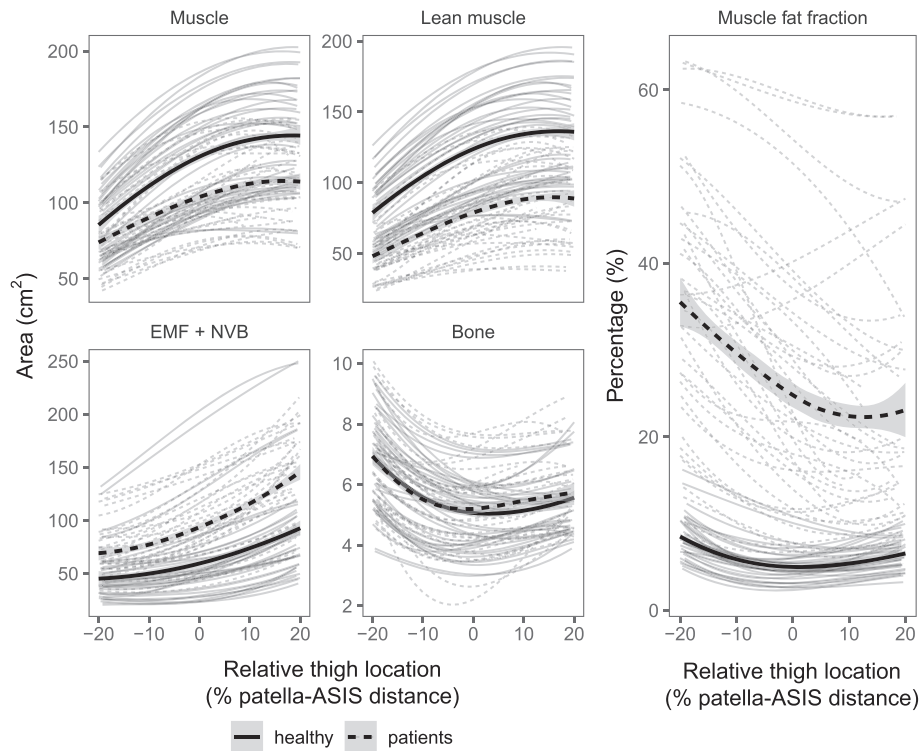


Figure 3 Regional thigh structure assessed using quantitative magnetic resonance imaging in healthy participants and patients with muscle disease. Areas of muscle, lean muscle, extramuscular fat and neurovascular bundles (EMF + NVB), bone, and muscle fat fraction according to relative thigh location expressed as a percentage of the distance between the upper edge of the patella and the anterior–superior iliac spine (patella–ASIS distance; with 0 corresponding to the central slice positioned at one-third of the patella–ASIS distance) as assessed using quantitative magnetic resonance imaging in healthy participants (solid grey lines for individuals, solid black line for group average) and patients with muscle disease (dashed grey lines for individuals, dashed black line for group average).

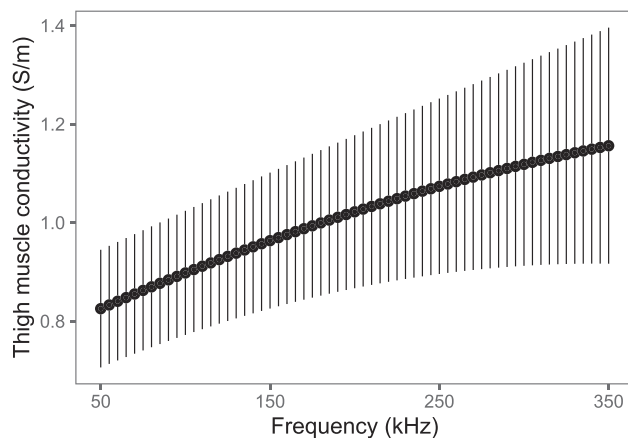


Figure 4 Newly computed muscle conductivity constant as a function of injected current frequency. The newly computed conductivity constant was computed using serial bioelectrical impedance analysis and quantitative muscle magnetic resonance imaging in the right thigh of half ($n = 10$) of healthy participants studied (see Methods section for more details). Data are shown as mean \pm standard deviation.

on Δ ICSA was found [$F(8, 36\ 875) = 103.34, P < 0.001$]. Post hoc tests revealed that Δ ICSA was significantly greater at relative thigh locations $\leq -10\%$ and $\geq 10\%$ of patella–ASIS distance

as compared with that observed at 0%. Δ ICSA according to the frequency of the injected current is shown in Figure 5B. A significant main effect of the frequency of the injected current on Δ ICSA was found [$F(60, 36\ 873) = 25.0, P < 0.001$]. Minimal Δ ICSA was 13.7% corresponding to measurements performed at 155 kHz. Post hoc tests revealed that Δ ICSA significantly differed from the minimal Δ ICSA at frequencies ≥ 270 kHz. Consistency between IV_{MRI} and IV_{BIA} at different frequencies is shown in Table 1. Δ ICSA was lower in the group of 10 healthy participants used to compute the conductivity constant ($10.1 \pm 6.9\%$) as compared with the healthy participants ($12.7 \pm 9.1\%$, difference in means = -2.6% ; $P < 0.01$).

Values of IV_{MRI} and IV_{BIA} at 155 kHz in patients and healthy participants are presented in Table 2. Agreement between IV_{BIA} at 155 kHz and V_{MRI} or IV_{MRI} is displayed on Figure 6. The mean absolute percentage difference between IV_{BIA} at 155 kHz and V_{MRI} was $14.1 \pm 13.5\%$ while the mean absolute percentage difference between IV_{BIA} at 155 kHz and IV_{MRI} (ΔIV) was $10.4 \pm 7.8\%$ (difference in means = -3.7% ; $P < 0.01$). There was a significant correlation between ΔIV and muscle FF ($R = 0.23, P < 0.05$, Figure 7B). There was no significant correlation between ΔIV and fat content in thigh expressed as a percentage of total thigh volume ($R = -0.19$,

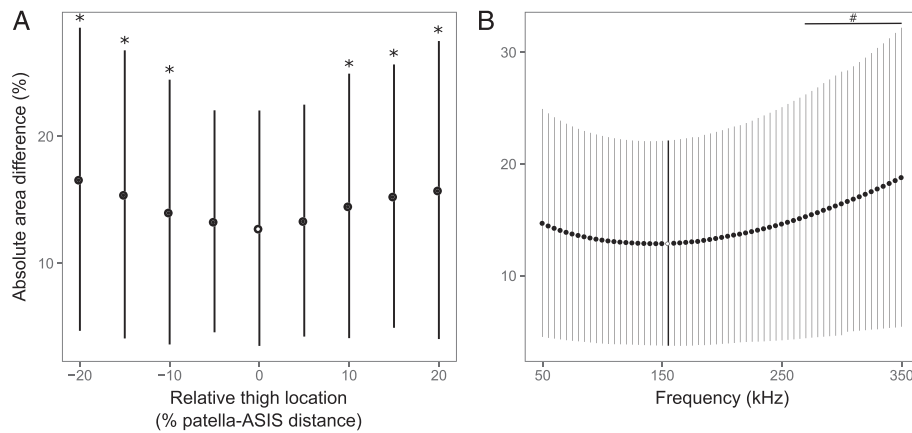


Figure 5 Absolute difference between lean muscle cross-sectional area estimated using serial bioelectrical impedance analysis and quantitative magnetic resonance imaging. Absolute difference between lean cross-sectional areas estimated using serial bioelectrical impedance analysis and magnetic resonance imaging as a function of relative thigh location expressed as a percentage of the distance between the upper edge of the patella and the anterior–superior iliac spine (patella–ASIS distance; with 0 corresponding to one-third of the patella–ASIS distance) (Panel A) and injected current frequency (Panel B). The minimum absolute area difference is highlighted in white in both panels. Data are shown as mean ± standard deviation. *Significantly different than absolute area difference compared with absolute area difference 0% relative thigh location. #Significantly different absolute area difference compared with absolute area difference obtained at 155 kHz.

Table 1 Regional lean muscle volume in thigh estimated using serial bioelectrical impedance analysis at multiple frequencies and using quantitative magnetic resonance imaging (n = 76)

Frequency (kHz)	IV _{MRI} (cm ³)	IV _{BIA} (cm ³)	P value	DIM (cm ³) [95% CI]	SEM (cm ³) [95% CI]	SEM (%) [95% CI]	LOA (cm ²) [lower upper]	ICC [95% CI]
50	1707 ± 732	1862 ± 800	<0.001	155 [108, 202]	144 [124, 172]	9.2 [7.9, 11.0]	[-254, 487]	0.95 [0.92, 0.96]
100	1707 ± 732	1823 ± 794	<0.001	116 [73, 160]	133 [115, 160]	8.0 [6.9, 9.6]	[-271, 469]	0.96 [0.94, 0.97]
150	1707 ± 732	1805 ± 791	<0.001	98 [55, 142]	133 [115, 159]	8.0 [6.9, 9.6]	[-273, 469]	0.96 [0.94, 0.97]
155 ^a	1707 ± 732	1804 ± 791	<0.001	97 [54, 141]	133 [115, 159]	8.1 [7.0, 9.7]	[-254, 487]	0.96 [0.94, 0.97]
200	1707 ± 732	1803 ± 791	<0.001	96 [50, 143]	142 [122, 169]	8.9 [7.7, 10.7]	[-297, 491]	0.96 [0.94, 0.97]
250	1707 ± 732	1819 ± 798	<0.001	112 [58, 166]	164 [141, 196]	10.8 [9.3, 12.9]	[-344, 569]	0.94 [0.92, 0.96]
300	1707 ± 732	1852 ± 815	<0.001	145 [79, 212]	202 [174, 241]	13.9 [11.9, 16.5]	[-416, 707]	0.92 [0.88, 0.94]
350	1707 ± 732	2023 ± 817	<0.001	212 [120, 304]	264 [225, 319]	18.0 [15.4, 21.8]	[-521, 945]	0.84 [0.77, 0.89]

CI, confidence interval; DIM, difference in means; ICC, intra-class correlation coefficient; LOA, limits of agreement; IV_{BIA}, lean muscle volume as estimated using serial bioelectrical impedance analysis; IV_{MRI}, lean muscle volume as assessed using magnetic resonance imaging; SEM, standard error of measurement.

^aIndicates the injected current frequency at which absolute difference between serial bioelectrical impedance analysis and magnetic resonance imaging in lean muscle cross-sectional areas was minimal (Figure 5B).

P = 0.1; R = 0.22, P = 0.07; Figure 7A and 7C, respectively). A significant effect of group (i.e. patients vs. healthy participants) was found on ΔIV with significantly smaller differences in healthy participants compared with patients (-5.9%, P < 0.001). Agreement between IV_{MRI} and IV_{BIA} when using five-electrode and three-electrode measurements at 155 kHz is shown in Table 3. There was no significant main effect of the number of electrodes on ΔIV [F(2, 144) = 2.11, P = 0.12].

Between-day reproducibility of serial bioelectrical impedance analysis estimates of lean muscle volume in thigh

Between-day reproducibility of IV_{BIA} in healthy subjects according to frequency and to the number of voltage

electrode used for measurements is shown in Table 4 and Figure 8. When looking at frequencies 50, 100, 150, 200, 250, 300, and 350 kHz, there was a significant main effect of the frequency on between-day differences in IV_{BIA} [F(6, 66) = 9.61, P < 0.001]. Post hoc tests revealed a significant difference in between-day differences in IV_{BIA} between 350 kHz and all other frequencies and between 300 kHz and 50, 100, and 150 kHz. When looking at estimates obtained at 155 kHz, we also found a significant main effect of the number of electrodes on absolute between-day percentage differences in IV_{BIA} [F(2, 22) = 4.21, P < 0.05]. Post hoc tests revealed a significant difference in between-day percentage differences in IV_{BIA} using three vs. all electrodes (13.9%, P < 0.05) and no difference between three vs. five (6.8%, P = 0.51) and five vs. all electrodes (6.8%, P = 0.46).

Table 2 Regional lean muscle volume in thigh estimated using serial bioelectrical impedance analysis and using quantitative magnetic resonance imaging in healthy participants ($n = 20$) and in patients ($n = 18$)

Group	IV _{MRI} (cm ³)	IV _{BIA} (cm ³)	<i>P</i> value	DIM (cm ³) [95% CI]	SEM (cm ³) [95% CI]	SEM (%) [95% CI]	ICC [95% CI]
Healthy	2090 ± 683	2171 ± 773	<0.05	80 [14, 146]	145 [119, 187]	6.2 [5.1, 8.0]	0.95 [0.92, 0.97]
Patients ^a	1255 ± 494	1373 ± 570	<0.001	118 [59, 176]	118 [95, 156]	9.4 [7.6, 12.4]	0.93 [0.88, 0.96]

CI, confidence interval; DIM, difference in means; ICC, intra-class correlation coefficient; IV_{BIA}, lean muscle volume estimated using serial bioelectrical impedance measurements performed at 155 kHz; IV_{MRI}, lean muscle volume as assessed using magnetic resonance imaging; SEM, standard error of measurement.

^aIndicates significantly greater absolute percentage difference between IV_{MRI} and IV_{BIA} in patients as compared with that observed in healthy participants ($P < 0.001$).

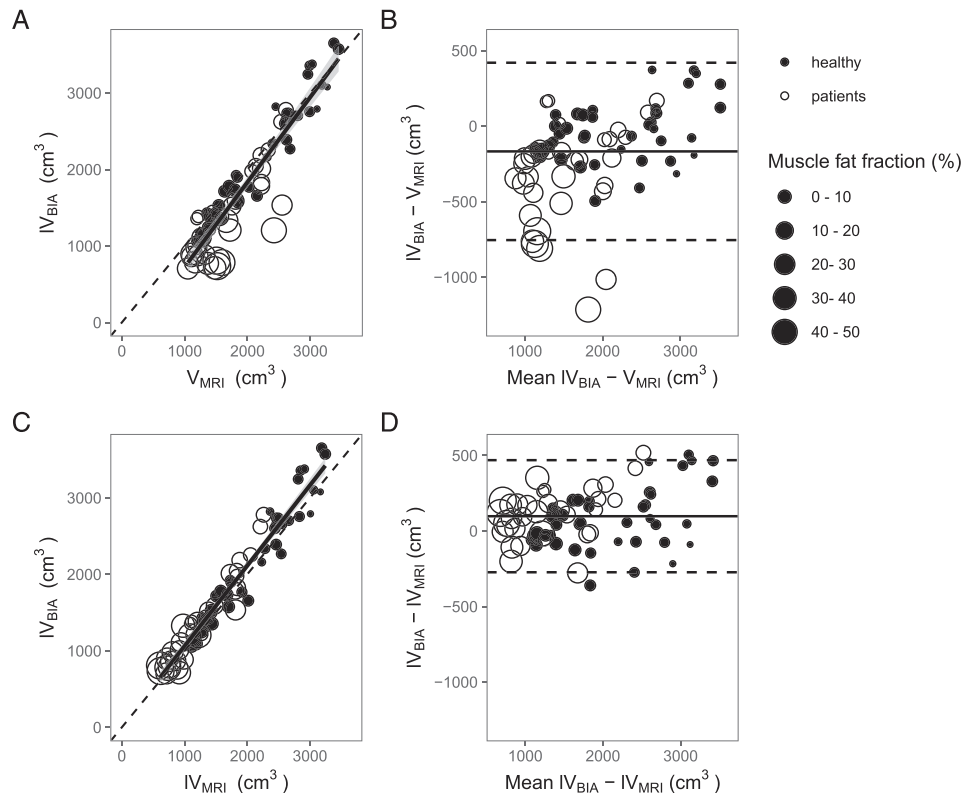


Figure 6 Agreement of regional lean muscle volume in thigh estimated using serial bioelectrical impedance analysis and quantitative magnetic resonance imaging (MRI). Regression analysis (Panels A and C) and Bland–Altman plots (Panels B and D) of thigh lean muscle volume estimated using serial bioelectrical impedance analysis (IV_{BIA}) performed at 155 kHz against whole and lean muscle volume assessed using quantitative MRI (V_{MRI} and IV_{MRI}, upper and lower panels, respectively). In (A) and (C), the dashed line represents the identity line, and the solid line indicates the linear regression line. In (B) and (D), the solid line indicates the difference in means between the measurements, and the dashed lines indicate the limits of agreement. Muscle fat fraction as assessed with quantitative MRI is indicated by marker size. One may note larger difference between MRI and serial bioelectrical impedance analysis when intramuscular fat is not taken into account.

Discussion

Regional thigh structure as assessed using quantitative magnetic resonance imaging

Healthy participants and patients exhibited heterogeneous areas of whole muscle, lean muscle, subcutaneous fat associated with neurovascular bundles as assessed using quantitative MRI. As expected, muscle FF was low in healthy participants and moderate to high in patients. These results

are in line with previously reported data in healthy participants²⁶ and patients with myopathies.²⁷

Muscle conductivity constant

As mentioned earlier, the value of the muscle conductivity constant is critical for the explanatory models used in the current work.^{8,16,17} The electrical properties of biological tissues have been extensively studied, mostly using macroscopic

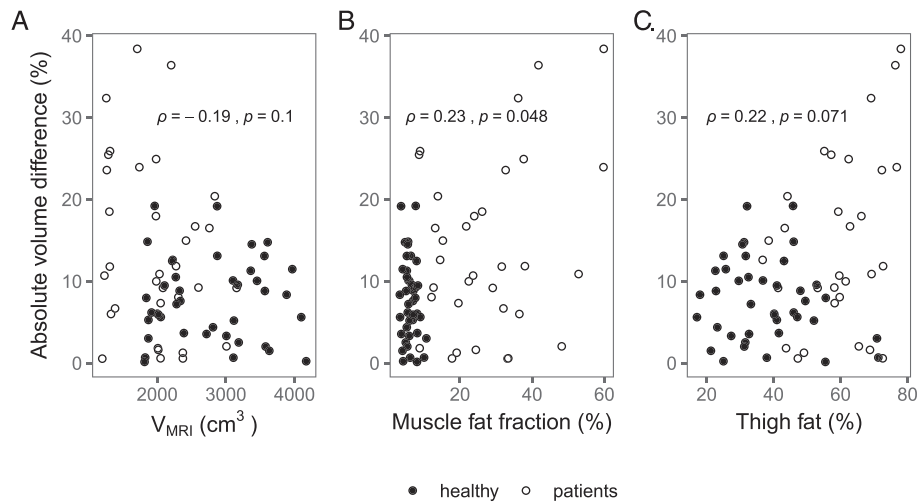


Figure 7 Absolute difference between regional lean muscle volume in thigh estimated using serial bioelectrical impedance analysis according to muscle volume, muscle fat fraction, and thigh fat percentage as assessed using quantitative magnetic resonance imaging (MRI). Magnitude of difference between regional lean muscle volume in thigh obtained using serial bioelectrical impedance analysis according to muscle volume (Panel A), muscle fat fraction (Panel B), and fat content in thigh fat expressed as a percentage of total thigh volume (Panel C) as assessed using quantitative MRI. Lean regional muscle volumes estimated using serial bioelectrical impedance measurements performed at 155 kHz were used (see Results section for more details).

Table 3 Regional lean muscle volume in thigh assessed by serial bioelectrical impedance analysis using five and three voltage electrode measurements along the thigh ($n = 76$)

n electrodes	Location (%)	IV_{MRI} (cm^3)	IV_{BIA} (cm^3)	P value	DIM (cm^3) [95% CI]	SEM (cm^3) [95% CI]	SEM (%) [95% CI]	ICC [95% CI]
All	-20 to 20	1707 ± 732	1804 ± 791	<0.001	97 [54, 141]	133 [115, 159]	8.1 [7.0, 9.7]	0.96 [0.94, 0.97]
5	-15 to 15	1339 ± 566	1336 ± 584	0.866	-3 [-41, 35]	117 [101, 140]	8.9 [7.6, 10.6]	0.96 [0.94, 0.97]
3	-7 to 7	646 ± 263	634 ± 292	0.337	-11 [-35, 12]	73 [63, 87]	10.9 [9.4, 13.0]	0.93 [0.90, 0.95]

n electrodes denotes the number of thigh voltage electrodes used for measurements; location (%) denotes the region of the thigh for which lean muscle volume was computed expressed as a percentage of the distance between the upper edge of the patella and the anterior–superior iliac spine with 0 corresponding to the central slice positioned at one-third of the patella–anterior–superior iliac spine distance. CI, confidence interval; DIM, difference in means; ICC, intra-class correlation coefficient; IV_{BIA} , lean muscle volume as estimated using serial bioelectrical impedance measurements performed at 155 kHz; IV_{MRI} , lean muscle volume as assessed using magnetic resonance imaging; SEM, standard error of measurement.

approaches.^{18,28} The specific conductivity of tissues depends on the frequency and the orientation of the tissue relative to the applied electrical field. The latter phenomenon, known as directional anisotropy, is highly prominent in the skeletal muscle as a consequence of its ultrastructure, that is, very long tubular cells with a variable three-dimensional arranged according to functional demands.²⁹ As a result, muscle conductivity along the muscle fibre length is substantially greater than across them. Because the thigh is composed of multiple muscles exhibiting various types of structure (e.g. pennation angles and shape), it is anticipated that the muscle conductivity constant obtained *in vitro* parallel to myofibres may not provide satisfactory results.³⁰ In previous S_{BIA} studies, conductivity constants from the aforementioned literature were used for analysis.^{15–17} In the present work, we computed a specific conductivity constant for the thigh while assuming that intramuscular fat, extramuscular fat, and bone had negligible conductivity (i.e. previous studies^{13,31}). The newly computed

conductivity constant was in the range of previously reported data for muscle conductivity assessed *in vitro*. For instance, the newly computed constant at 50 kHz was 0.82 S/m vs. 0.85 S/m in Zheng *et al.*¹⁹ This slightly smaller constant may be explained, at least in part, by the fact that conductivity was measured parallel to muscle fibres in Zheng *et al.*¹⁹ As expected, the conductivity constant increased according to injected current frequency as a result of the reduction of cellular membrane capacitance.¹⁸

Effect of location and frequency on estimates of lean regional muscle volume using serial bioelectrical impedance analysis

We found a small albeit significant effect of measurement location on the absolute difference in lean muscle cross-sectional areas estimated using S_{BIA} and MRI (Figure

Table 4 Between-day reproducibility of regional lean muscle volume in thigh estimated using serial bioelectrical impedance analysis according to frequency and to the number of voltage electrode measurements ($n = 12$)

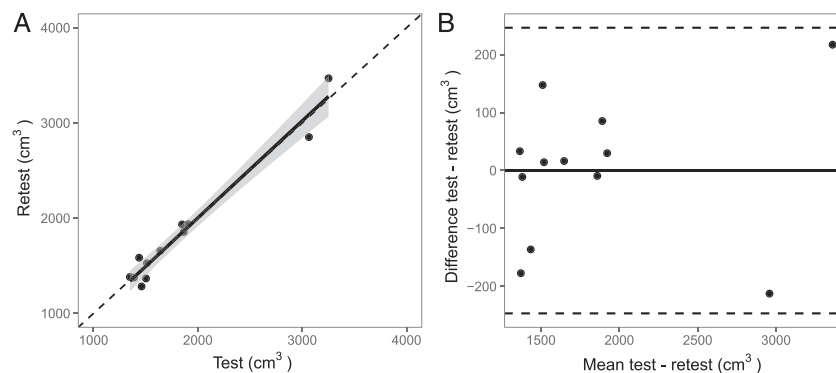
	Location (%)	Day 1 (cm ³)	Day 2 (cm ³)	<i>P</i> value	DIM (cm ³) [95% CI]	SEM (cm ³) [95% CI]	SEM (%) [95% CI]	ICC [95% CI]
Frequency (kHz)								
50 ^{a,b}	—	1853 ± 560	1809 ± 569	0.124	-44 [-102, 14]	65 [46, 110]	4.1 [2.9, 6.9]	0.98 [0.96, 0.99]
100 ^{a,b}	—	1842 ± 599	1815 ± 616	0.369	-26 [-88, 36]	69 [49, 117]	3.9 [2.8, 6.6]	0.99 [0.97, 1.00]
150 ^{a,b}	—	1850 ± 636	1848 ± 660	0.943	-3 [-81, 75]	87 [62, 147]	4.5 [3.2, 7.6]	0.98 [0.96, 0.99]
200 ^a	—	1882 ± 681	1905 ± 709	0.629	22 [-77, 122]	111 [78, 188]	5.5 [3.9, 9.3]	0.98 [0.94, 0.99]
250 ^a	—	1943 ± 743	1992 ± 786	0.449	49 [-88, 185]	152 [108, 258]	7.2 [5.1, 12.2]	0.96 [0.90, 0.99]
300 ^a	—	2040 ± 839	2122 ± 924	0.401	83 [-126, 291]	232 [164, 393]	10.1 [7.5, 17.9]	0.93 [0.83, 0.98]
350	—	2176 ± 998	2322 ± 1189	0.377	146 [-203, 495]	389 [275, 660]	18.2 [12.1, 30.3]	0.88 [0.70, 0.95]
<i>n</i> electrodes								
All	-20 to 20	1852 ± 640	1852 ± 664	0.997	0 [-80, 79]	88 [62, 150]	4.6 [3.2, 7.8]	0.98 [0.95, 0.99]
5	-15 to 15	1391 ± 488	1386 ± 476	0.915	-5 [-124, 112]	132 [93, 224]	11.9 [8.3, 20.1]	0.93 [0.82, 0.97]
3 ^c	-7 to 7	636 ± 214	678 ± 230	0.404	41 [-64, 147]	117 [83, 200]	20.8 [14.7, 35.3]	0.73 [0.40, 0.89]

The effect of frequency on between-day reproducibility using measurements performed using all electrodes is presented. The effect of the number of electrodes used (*n* electrodes) using measurements performed at 155 kHz is displayed; *n* electrodes denotes the number of thigh voltage electrodes used for measurements; location (%) denotes the region of the thigh for which lean muscle volume was computed expressed as a percentage of the distance between the upper edge of the patella and the anterior–superior iliac spine with 0 to one-third of the patella–anterior–superior iliac spine distance. CI, confidence interval; DIM, difference in means; ICC, intra-class correlation coefficient; SEM, standard error of measurement.

^aIndicates significantly larger difference between Day 1 and Day 2 in measurements performed at 350 kHz.

^bIndicates significantly larger difference between Day 1 and Day 2 in measurements performed at 300 kHz.

^cIndicates significantly larger difference between Day 1 and Day 2 as compared with that observed using all electrodes ($P < 0.05$).

**Figure 8** Between-day reproducibility of regional lean muscle volume in thigh estimated using serial bioelectrical impedance analysis. Regression analysis (Panel A) and Bland–Altman plots (Panel B) of thigh lean muscle volume estimated using serial bioelectrical impedance measurements performed at 155 kHz on two different occasions. In (A), the dashed line represents the identity line, and the solid line indicates the linear regression line. In (B), the solid line indicates the difference in means between the measurements, and the dashed lines indicate the limits of agreement.

5A). Differences between lean muscle volume assessed using S_{BIA} and MRI were also found to increase significantly at frequencies >270 kHz (Figure 5B). As directional anisotropy is known to decrease according to injected current frequency,¹⁸ one may expect a lower relative error at higher frequencies when using a conductivity constant that has been obtained *in vitro* parallel to muscle fibres. Consistently, Stahn *et al.*¹⁷ reported a lower relative error at 500 kHz as compared with 50 kHz. However, conductivity constants used for 50 and 500 kHz measurements seemed to originate from two distinct studies,^{19,30} hindering the interpretation of these findings. In the present study, the influence of directional anisotropy was partially ruled out as the computation of the conductivity

constant was experimentally derived from anatomical muscle cross-sectional areas. In other words, conductivity was measured assuming a dominant direction of myofibres relative to the current flow within thigh muscles for each investigated frequency. However, we observed a large difference in the conductivity constant at high frequencies that may explain, at least in part, larger absolute volume differences at higher frequencies. The error in the measurement of the real part of the impedance value at higher frequencies related to the bioimpedance device used may also contribute to explain these findings.³² Based on our findings, no advantage of multifrequency S_{BIA} acquisition has emerged when using this type of BIA explanatory models. Using a single frequency (for instance, around 150 kHz)

may substantially reduce the duration of acquisitions and thus limit confounding factors such as movements of the subject. At last, the fact that the conductivity constant was computed and averaged over all thigh locations that display different muscle organization may also contribute to explain the effect of measurement location on Δ ICSA.

Agreement between serial bioelectrical impedance analysis and quantitative magnetic resonance imaging for estimating regional lean muscle volume in thigh

Our data showed strong agreement between IV_{BIA} and V_{MRI} as indicated by SEM < 10% and ICC > 0.9 in both healthy participants with variable BMI and patients with muscle atrophy and fatty infiltration. We also found that IV_{BIA} tended to be larger than IV_{MRI} . There are several potential explanations for these findings. Both extramuscular fat and intramuscular fat were assumed to have a negligible effect on resistance measurements because of the very low conductivity of fat (~0.06 S/m at 50 kHz vs. ~0.85 S/m in muscle according to the study of Brown *et al.*¹³). However, the conductivity of neurovascular bundles has been reported to be comparable with that of muscle (0.63 S/m at 50 kHz), and it may thus substantially influence resistance measurements. As neurovascular bundles may be difficult to delineate on MRI images, this was not performed systematically in the present work (i.e. subcutaneous fat, intermuscular fat, and neurovascular bundles were not segmented independently). We segmented neurovascular bundles on the central slices of four subjects (including two healthy participants and two patients). The area of neurovascular bundles was, on average, 3 cm² as compared with a mean lean muscle area of 72 cm² that is approximately 3%. This emphasizes that neurovascular bundles may substantially contribute to the overestimation of IV_{BIA} , as previously reported.^{13,14} Another potential explanation is related to the fact that the newly computed conductivity constant originated from a subsample of healthy participants, as illustrated by the slight, yet significant, difference with the healthy subjects whom data have not been used to compute the conductivity constant. More interestingly, ΔIV was found to be larger in patients compared with healthy participants. A potential explanation is that patients exhibit a very different thigh composition and thigh muscle structure (e.g. different global pennation angles and overall limb fat content) as opposed to their healthy counterparts, resulting in conductivity constants that may be imperfectly suited to IV_{BIA} measurements in patients. However, the absence of strong relationships between ΔIV and V_{MRI} and thigh fat expressed as a percentage of total thigh volume do not support this hypothesis (Figure 7A and 7C). Conversely, and although this relationship was weak, patients with the highest muscle fatty infiltration had higher ΔIV . One potential

explanation is that delineating muscle compartment on MRI images may become particularly arduous in patients with very severe fatty degeneration that might have led to imprecision in the estimation of IV_{MRI} . Patients with most severe muscle degeneration may also be more likely to present oedema that may bias S_{BIA} measurements.³³ Noteworthy, oedema would also bias measurements of IV_{MRI} .

Our results showed that reliable estimates of regional lean thigh SMV may be obtained using five electrodes (i.e. corresponding to 20 cm length). Interestingly, there was no overestimation of lean thigh SMV values when using five or three electrodes (Table 3). This relates, at least in part, to the larger difference in Δ ICSA observed on most distal and most proximal S_{BIA} measurements (Figure 5A). There are several potential explanations for this phenomenon. Distally, the muscle compartment is not predominant so that assumptions of the model may be violated. Proximally, the measurement of resistance may be parasitized by the lower trunk. When using three electrodes only, the precision of estimates was slightly reduced, likely due to imperfect fitting of the relative resistance profiles.

Between-day reproducibility of lean muscle volume estimated using serial bioelectrical impedance analysis

Both absolute and relative between-day reproducibility of IV_{BIA} were good as supported by SEM < 6% and ICC > 0.9 between 50 and 200 kHz. This is in line with previous reports regarding the between-day reproducibility of methods such as quantitative MRI for assessing lean regional SMV, although quantitative MRI may provide very reproducible estimates in healthy subjects.³⁴ Very interestingly, our results showed that between-day reproducibility was increasingly impaired above 200 kHz. These findings may contribute to explain the largest difference observed between S_{BIA} and MRI at high frequencies mentioned earlier. Previously identified factors such as electrode impedance mismatch and the effect of stray capacitance may contribute to explain these impairments in agreement between S_{BIA} and MRI as well as impairments in reproducibility at high frequencies. Correction techniques have been proposed to reduce these artefacts^{35,36} and could be implemented to further investigate the potential of multifrequency S_{BIA} . Although non-significant, between-day variability of IV_{BIA} measurements with five electrodes appeared to be higher as compared with assessments using all electrodes (SEM < 13% and ICC > 0.8) and even more increased when employing three electrodes (SEM < 24% and ICC > 0.5). These findings support that lean thigh muscle volume as assessed with S_{BIA} is reproducible between sessions and acceptable when using five instead of all electrodes. Using five electrodes can facilitate the implementation of S_{BIA} for the assessment of lean regional SMV in longitudinal studies.

Limitations

This work has several limitations. First, the sample size of both healthy participants and patients was limited. A larger sample size, in particular when considering the wide BMI range in healthy participants, may help to further refine the accuracy and generalization of the conductivity constant. Second, between-day reproducibility in patients, as well as sensitivity to changes, remains to be investigated. Third, as it is the case with traditional BIA methods, fluid changes may substantially affect estimates,³³ potentially limiting the use of the method in contexts associated with large fluctuations in fluid balance.³⁷ Postural effects on fluid distribution may be easily circumvented by allowing 10 min resting periods before measurements.⁸ Fourth, S_{BIA} measurements do not allow assessment of individual muscle volume and pathophysiological changes occurring within muscles such as fatty degeneration. However, it appears to be very promising when regional lean SMV assessments are pursued. Other local BIA approaches that might allow the estimation of pathophysiological changes are currently emerging.¹² Combining S_{BIA} with these approaches might be promising to obtain both quantitative and qualitative insights regarding muscle status. Future research will include the acquisition of more data in a broader scope of diseases involving both primary and secondary muscle impairments. Another limitation is that not all available MRI slices were segmented. Conversely, segmenting a reduced number of slices has been shown to provide precise estimates of regional SMV.²³ Increasing the density of electrodes (i.e. number of electrodes on a given length) might also help to improve estimations by facilitating the fitting of the relative resistance profiles. Similar works shall be conducted in legs and upper limbs.¹⁷ The ability of S_{BIA}

to monitor change in regional SMV over time and/or in response to interventions will be investigated in future studies.

Conclusions

This study demonstrates a strong agreement between lean regional SMV estimated using S_{BIA} and quantitative MRI both in healthy subjects and in patients with muscle wasting and fatty degeneration. S_{BIA} shows promises for non-invasive, fast, and accessible estimation and follow-up of lean regional muscle volume in transversal and longitudinal studies.

Acknowledgements

We gratefully thank all the volunteers who participated in this study. This study was supported by Association Française Contre Les Myopathies (AFM). We also thank the Bioparhom society for technical support and kind help when setting up this experiment. The authors of this manuscript certify that they comply with the ethical guidelines for authorship and publishing in the *Journal of Cachexia, Sarcopenia and Muscle*.³⁸

Conflict of interest

The authors have no conflict of interest to disclose.

References

- García-Hermoso A, Cavero-Redondo I, Ramírez-Vélez R, Ruiz JR, Ortega FB, Lee DC, et al. Muscular strength as a predictor of all-cause mortality in apparently healthy population: a systematic review and meta-analysis of data from approximately 2 million men and women. *Arch Phys Med Rehabil* 2018;**99**: 2100–2113.e5.
- Maeda K, Akagi J. Muscle mass loss is a potential predictor of 90-day mortality in older adults with aspiration pneumonia. *J Am Geriatr Soc* 2017;**65**:e18–e22.
- Brown JC, Harhay MO, Harhay MN. Appendicular lean mass and mortality among prefrail and frail older adults. *J Nutr Health Aging* 2017;**21**:342–345.
- Buckinx F, Landi F, Cesari M, Fielding RA, Visser M, Engelke K, et al. Pitfalls in the measurement of muscle mass: a need for a reference standard. *J Cachexia Sarcopenia Muscle* 2018;**9**:269–278.
- Borga M, West J, Bell JD, Harvey NC, Romu T, Heymsfield SB, et al. Advanced body composition assessment: from body mass index to body composition profiling. *J Invest Med* 2018;**66**:1–9.
- Cruz-Jentoft AJ, Baeyens JP, Bauer JM, Boirie Y, Cederholm T, Landi F, et al. Sarcopenia: European consensus on definition and diagnosis: report of the European Working Group on Sarcopenia in Older People. *Age Ageing* 2010;**39**:412–423.
- Yamada Y. Muscle mass, quality, and composition changes during atrophy and sarcopenia. In Xiao J, ed. *Muscle Atrophy*. Singapore: Springer Singapore; 2018. p 47–72.
- Stahn A, Terblanche E, Gunga H-C. Use of bioelectrical impedance: general principles and overview. In Preedy VR, ed. *Handbook of Anthropometry: Physical Measures of Human Form in Health and Disease*. New York, NY: Springer New York; 2012. p 49–90.
- Janssen I, Heymsfield SB, Baumgartner RN, Ross R. Estimation of skeletal muscle mass by bioelectrical impedance analysis. *J Appl Physiol (1985)* 2000;**89**:465–471.
- Kyle UG, Bosaeus I, De Lorenzo AD, Deurenberg P, Elia M, Gómez JM, et al. Bioelectrical impedance analysis—part I: review of principles and methods. *Clin Nutr* 2004;**23**:1226–1243.
- Roy B, Rutkove SB, Nowak RJ. Electrical impedance myography as a biomarker of inclusion body myositis: a cross-sectional study. *Clin Neurophysiol* 2020;**131**: 368–371.
- Rutkove SB, Sanchez B. Electrical impedance methods in neuromuscular assessment: an overview. *Cold Spring Harb Perspect Med* 2019;**9**:a034405.
- Brown BH, Karatzas T, Nakielny R, Clarke RG. Determination of upper arm muscle

- and fat areas using electrical impedance measurements. *Clin Phys Physiol Meas* 1988;**9**:47–55.
14. Fuller NJ, Hardingham CR, Graves M, Screaton N, Dixon AK, Ward LC, et al. Predicting composition of leg sections with anthropometry and bioelectrical impedance analysis, using magnetic resonance imaging as reference. *Clin Sci (Lond)* 1999;**96**:647–657.
 15. Salinari S, Bertuzzi A, Mingrone G, Capristo E, Pietrobelli A, Campioni P, et al. New bioimpedance model accurately predicts lower limb muscle volume: validation by magnetic resonance imaging. *Am J Physiol Endocrinol Metab* 2002;**282**:E960–E966.
 16. Salinari S, Bertuzzi A, Mingrone G, Capristo E, Scarfone A, Greco AV, et al. Bioimpedance analysis: a useful technique for assessing appendicular lean soft tissue mass and distribution. *J Appl Physiol (1985)* 2003;**94**:1552–1556.
 17. Stahn A, Terblanche E, Strobel G. Modeling upper and lower limb muscle volume by bioelectrical impedance analysis. *J Appl Physiol (1985)* 2007;**103**:1428–1435.
 18. Miklavčič D, Pavšelj N, Hart FX. Electric properties of tissues. In *Wiley Encyclopedia of Biomedical Engineering*; 2006.
 19. Zheng E, Shao S, Webster JG. Impedance of skeletal muscle from 1 Hz to 1 MHz. *IEEE Trans Biomed Eng* 1984;**31**:477–481.
 20. Gabriel S, Lau RW, Gabriel C. The dielectric properties of biological tissues: II. Measurements in the frequency range 10Hz to 20GHz. *Phys Med Biol* 1996;**41**:2251–2269.
 21. Gielen FL, Wallinga-de Jonge W, Boon KL. Electrical conductivity of skeletal muscle tissue: experimental results from different muscles in vivo. *Med Biol Eng Comput* 1984;**22**:569–577.
 22. Azzabou N, Loureiro de Sousa P, Caldas E, Carlier PG. Validation of a generic approach to muscle water T2 determination at 3T in fat-infiltrated skeletal muscle. *J Magn Reson Imaging* 2015;**41**:645–653.
 23. Barnouin Y, Butler-Browne G, Moraux A, Reversat D, Leroux G, Béhin A, et al. Comparison of different methods to estimate the volume of the quadriceps femoris muscles using MRI. *J Med Imaging Health Inform* 2015;**5**:1201–1207.
 24. Gidaro T, Reyngoudt H, Le Louër J, Behin A, Toumi F, Villeret M, et al. Quantitative nuclear magnetic resonance imaging detects subclinical changes over 1 year in skeletal muscle of GNE myopathy. *J Neurol* 2020;**267**:228–238.
 25. Team RC. R: a language and environment for statistical computing 2017.
 26. Hogrel JY, Barnouin Y, Azzabou N, Butler-Browne G, Voit T, Moraux A, et al. NMR imaging estimates of muscle volume and intramuscular fat infiltration in the thigh: variations with muscle, gender, and age. *Age (Dordr)* 2015;**37**:9798.
 27. Morrow JM, Sinclair CD, Fischmann A, Machado PM, Reilly MM, Yousry TA, et al. MRI biomarker assessment of neuromuscular disease progression: a prospective observational cohort study. *Lancet Neurol* 2016;**15**:65–77.
 28. Nagy JA, DiDonato CJ, Rutkove SB, Sanchez B. Permittivity of ex vivo healthy and diseased murine skeletal muscle from 10 kHz to 1 MHz. *Sci Data* 2019;**6**:37.
 29. Lieber RL, Ward SR. Skeletal muscle design to meet functional demands. *Philos Trans R Soc Lond B Biol Sci* 2011;**366**:1466–1476.
 30. Aaron R, Huang M, Shiffman CA. Anisotropy of human muscle via non-invasive impedance measurements. *Phys Med Biol* 1997;**42**:1245–1262.
 31. Barber DC, Brown BH. Applied potential tomography. *J Br Interplanet Soc* 1989;**42**:391–393.
 32. Bogonez-Franco P, Nescolarde L, McAdams E, Rosell-Ferrer J. Multifrequency right-side, localized and segmental BIA obtained with different bioimpedance analysers. *Physiol Meas* 2015;**36**:85–106.
 33. Scharfetter H, Monif M, László Z, Lambauer T, Hutten H, Hinghofer-Szalkay H. Effect of postural changes on the reliability of volume estimations from bioimpedance spectroscopy data. *Kidney Int* 1997;**51**:1078–1087.
 34. Pons C, Borotikar B, Garetier M, Burdin V, Ben Salem D, Lempereur M, et al. Quantifying skeletal muscle volume and shape in humans using MRI: a systematic review of validity and reliability. *PLoS ONE* 2018;**13**:e0207847.
 35. Buendia R, Seoane F, Gil-Pita R. A novel approach for removing the hook effect artefact from Electrical Bioimpedance spectroscopy measurements. *J Phys: Conf Series* 2010;**224**:012126.
 36. Montalibet A, McAdams E. A practical method to reduce electrode mismatch artefacts during 4-electrode bioimpedance spectroscopy measurements. *Annu Int Conf IEEE Eng Med Biol Soc* 2018;**5775**–5779.
 37. Nakanishi N, Tsutsumi R, Okayama Y, Takashima T, Ueno Y, Itagaki T, et al. Monitoring of muscle mass in critically ill patients: comparison of ultrasound and two bioelectrical impedance analysis devices. *J Intensive Care* 2019;**7**:61–61.
 38. von Haehling S, Morley JE, Coats AJS, Anker SD. Ethical guidelines for publishing in the Journal of Cachexia, Sarcopenia and Muscle: update 2019. *J Cachexia Sarcopenia Muscle* 2019;**10**:1143–1145.